SUITABILITY OF $POCL_3$ DIFFUSION PROCESSES WITH IN-SITU OXIDATION FOR FORMING LASER-DOPED SELECTIVE EMITTERS WITH LOW CARRIER RECOMBINATION

S. Werner, E. Lohmüller, J. Weber, A. Wolf
Fraunhofer Institute for Solar Energy Systems ISE, Heidenhofstr. 2, 79110 Freiburg, Germany
Phone: +49 761 - 4588 5049; e-mail: sabrina.werner@ise.fraunhofer.de

ABSTRACT: Laser-doped selective emitters feature the advantage of more effective shielding of minority charge carriers from the metal contacts while allowing for low emitter saturation current density j_{0e} in the photoactive area. The formation of emitters by diffusion processes using phosphorus oxychloride ($POCl_3$) with incorporated in-situ oxidation gains more and more attention as it allows for low j_{0e} below 90 fA/cm² on textured surface with silicon nitride passivation in industrial cycle times. Hence, the combination of both—$POCl_3$ diffusion with in-situ oxidation and laser doping—is very interesting. We examine four different $POCl_3$ diffusions with in-situ oxidation and one reference $POCl_3$ diffusion without in-situ oxidation in terms of their suitability for selective emitter laser doping. Detailed characterizations of the grown layers on the silicon surface are performed after diffusion with respect to the individual layer thicknesses of the phosphosilicate glass (PSG) and the intermediate silicon dioxide (SiO_2) layer as well as the stacks' total phosphorus doses. The as-diffused depth-dependent charge carrier concentration profiles show that a second PSG deposition step attached after drive-in to the diffusion processes hardly impacts their course. We find that $POCl_3$ diffusions with in-situ oxidation—especially those with second deposition step—allow for effective laser doping. Thereby, the intermediate SiO_2 layer thickness plays a key role: the thicker the layer is the less phosphorus can be incorporated additionally from the PSG layer into the silicon.
Keywords: in-situ oxidation, $POCl_3$ diffusion, selective emitter, laser doping, phosphosilicate glass

1 INTRODUCTION

Tube furnace diffusion processes using phosphorus oxychloride ($POCl_3$) as liquid dopant precursor are the dominating emitter formation technology for p-type silicon solar cells [1]. Improving $POCl_3$ diffusion processes and the resulting emitter doping profiles is essential for further increasing the energy conversion efficiency of silicon solar cells. The reduction of emitter recombination, enabled by a fast progress in front contact screen printing paste properties, has been of major interest in the past few years.

An approach to realize less emitter recombination is the reduction of the surface doping concentration by implementing an in-situ oxidation into the $POCl_3$ diffusion process [2–9]. When applied to passivated emitter and rear solar cells (PERC) [10], energy conversion efficiencies beyond 21% are reported [6,11,12]. As the charge carrier recombination at the metal contacts is high for that kind of doping profiles with low surface doping concentration [13], one option for its decrease is the selective emitter approach.

Recently, selective emitters came back into focus for PERC solar cells targeting the 22% efficiency regime and above [6,11,12,14,15]. The selective emitter can be formed by, e.g., local laser doping out of the phosphosilicate glass (PSG) layer [16]. Correctly, $POCl_3$ diffusions form a stack layer consisting of a PSG layer and a silicon dioxide (SiO_2) layer: the SiO_2 layer separates the PSG layer from the silicon surface [9,8,17,18]. Hereby, the SiO_2 layer features a much lower phosphorus concentration than the phosphorus-rich PSG layer.

For laser doping, sufficiently high phosphorus content within this PSG/SiO_2 stack layer is necessary. Hence, this paper investigates the combination of tube furnace $POCl_3$ diffusion with in-situ oxidation and the formation of selective emitters by laser doping out of the grown PSG/SiO_2 stack layer.

2 APPROACH

The approach pursued in this paper to ensure sufficient phosphorus content in the PSG/SiO_2 stack layer for effective laser doping is the implementation of a second deposition step with active nitrogen (N_2) gas flow through the $POCl_3$ bubbler (i.e. active N_2-$POCl_3$ flow) at the end of the diffusion process.

We investigate two pairs of $POCl_3$ diffusion processes that feature an in-situ oxidation and that are performed with and without a second deposition step, respectively. $POCl_3$ diffusion without in-situ oxidation but second deposition step serves as reference. Table I summarizes the examined $POCl_3$ diffusion processes. Process details and the labeling of the processes are discussed in detail in section 2.1.

The schematic experiment plan in Fig. 1 depicts the three groups of test samples fabricated and the different characterization approaches applied in this work. Full-square p-type Czochralski-grown silicon (Cz-Si) wafers with an edge length of 156 mm serve as starting material. After either saw damage etching or alkaline texturing, the five different tube furnace $POCl_3$ diffusion processes form the emitter and the PSG/SiO_2 stack layer.

The different $POCl_3$ diffusion processes, the applied

Table I: Summary of the five investigated $POCl_3$ diffusion processes. The emitter dark saturation current densities j_{0e}, determined on alkaline textured surface after passivation by a conventional SiN_x layer and firing, are taken from Refs. [4,11,13]. (n.d.: not determined)

$POCl_3$ process	1st dep. (N_2-$POCl_3$)	drive-in (O_2 share)	2nd dep.	j_{0e} (fA/cm²)
Ref 2nd dep	med	< 4%	yes	42
in-situ thin	low	100%	-	73
in-situ thin 2nd dep	low	100%	yes	n.d.
in-situ thick	high	100%	-	85
in-situ thick 2nd dep	high	100%	yes	n.d.

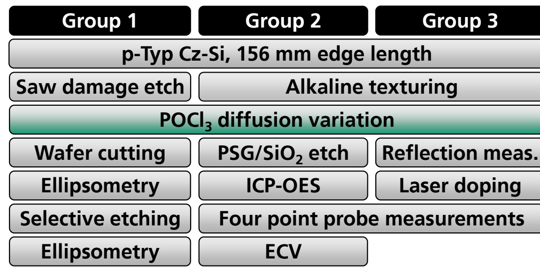

Figure 1: Experiment plan for investigating laser doping out of the SiO_2/PSG stack layer formed by different $POCl_3$ diffusion processes. (ECV: electrochemical capacitance-voltage measurements; ICP-OES: inductively coupled plasma optical emission spectrometry).

further process steps, and the utilized characterization methods are being discussed in the following sections.

2.1 $POCl_3$ diffusion processes

We target at low content of inactive phosphorus at the surface in the as-diffused emitter and thus, low charge carrier recombination in the homogeneously-doped area. For this purpose, we select the five $POCl_3$ diffusion processes summarized in Table I. For three of the five processes, we previously characterized their emitter dark saturation current density j_{0e} in Refs. [4,11,13]. The j_{0e} values on alkaline textured surface passivated by a conventional silicon nitride (SiN_x) passivation layer that is formed by plasma-enhanced chemical vapor deposition are found to be between 42 fA/cm² $\leq j_{0e} \leq$ 85 fA/cm² after simulated contact firing (see also Table I, rightmost column).

Table I also contains characteristic process parameters for the examined $POCl_3$ diffusion processes. We label the processes with respect to the used in-situ oxidation and the thickness of the resulting total PSG/SiO_2 stack layer. The reference process "Ref 2nd dep" has no in-situ oxidation as the oxygen (O_2) share in the gas atmosphere during drive-in is below 4% but features a second PSG deposition with active N_2-$POCl_3$ flow after the drive-in. For the other four processes, the drive-in with 100% O_2 share is similar. Corresponding to the name convention, the processes "in-situ thin" and "in-situ thick" feature either a thin or a thick PSG/SiO_2 stack layer after diffusion, respectively (see section 3.1). The N_2-$POCl_3$ and O_2 gas flows during the first deposition are a factor two to three lower for the process "in-situ thin" than for the process "in-situ thick". The suffix "2nd dep" indicates that a second PSG deposition step with active N_2-$POCl_3$ flow follows the drive-in step. The two process variations with the same second deposition step as used for the reference process are accordingly named "in-situ thin 2nd dep" and "in-situ thick 2nd dep".

2.2 Determination of layer thicknesses by means of selective etching

In order to extract the individual thicknesses of the PSG and SiO_2 layers formed during the five $POCl_3$ diffusions, the wafers with saw damage etched surface of group 1 in Fig. 1 are cut into 36 pieces each after diffusion. Ellipsometry measurements are performed before and after stepwise etching the stack layers in 0.1wt% hydrofluoric acid (HF) solution [9]. As the etching rate is dependent on the phosphorus concentration within the respective layer [8,9], the thickness of each layer can be extracted. The detailed procedure is described in Ref. [9].

Applying this procedure, we examine the individual thicknesses of the PSG and SiO_2 layers of the five diffusion processes and the impact of a second deposition step on these layer thicknesses for diffusion processes with in-situ oxidation.

2.3 Determination of phosphorus doses and charge carrier concentration profiles

We use the inductively coupled plasma optical emission spectrometry (ICP-OES) [19] to determine the phosphorus dose within the total PSG/SiO_2 stack layer on alkaline textured surfaces. Therefore, the stack layers of the wafers of group 2 in Fig. 1 are etched in diluted HF and the solution is analyzed with respect to its phosphorus concentration.

After the PSG/SiO_2 stack layer has been removed, the samples are further characterized with respect to their doping properties. Electrochemical capacitance-voltage measurements (ECV) [20] yield the charge carrier concentration profiles. The profiles are scaled to match the sheet resistances R_{sh} [13,21], which are locally determined by four point probe (4pp) measurements around the ECV spots.

2.4 Suitability for laser doping

To examine the suitability of the $POCl_3$ diffusion processes with respect to laser doping, we use a pulsed ultraviolet (UV) ns-laser with a wavelength λ_{laser} = 355 nm [22].

Subsequent to reflection measurements of the PSG/SiO_2 stack layer on textured surface for the wafers of group 3 in Fig. 1, we prepare 2 x 2 cm²-large test fields as shown in Fig. 2 applying four different pulse energies $E_{p,set}$ = {62 µJ; 74 µJ; 90 µJ; 120 µJ} at constant pulse-to-pulse and line-to-line distances d_{pulse} = 15 µm and d_{line} = 25 µm, respectively. Then, the evolution of R_{sh} for the applied laser processes for the different $POCl_3$ diffusions is determined by 4pp measurements.

3 RESULTS

3.1 PSG/SiO_2 layer thicknesses after $POCl_3$ diffusion

Fig. 3 shows the individual thicknesses of the PSG and SiO_2 layers d_{PSG} and d_{SiO2}, respectively, for the five diffusion processes investigated in this work.

For the reference process "Ref 2nd dep", the PSG layer with d_{PSG} = (24 ± 2) nm is about four times thicker than the SiO_2 layer with d_{SiO2} = (6 ± 1) nm. Chen et al. [18] reported a nearly constant SiO_2 layer thickness $d_{SiO2} \approx$ 6 nm for different deposition times and $POCl_3$ flow rates for common diffusion processes without in-situ oxidation, while they found the total stack layer thicknesses d

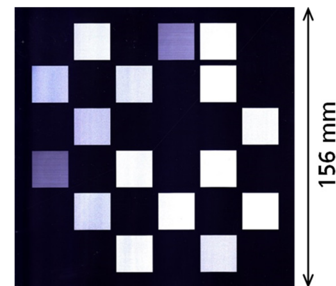

Figure 2: Image scan of an alkaline textured Cz-Si wafer with PSG/SiO_2 stack layer after laser doping. The visible square fields with a size of 2 x 2 cm² were processed with different laser parameters.

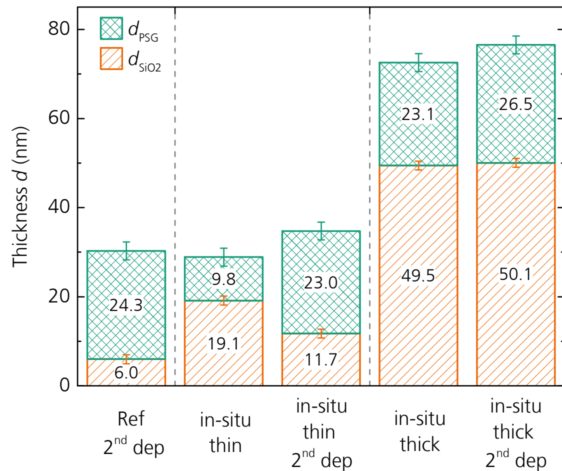

Figure 3: Individual layer thicknesses d_{PSG} and d_{SiO2} of the PSG and the SiO_2 layer, respectively, formed on the silicon surface during the five $POCl_3$ tube furnace diffusions from Table I. The individual thicknesses are extracted by the selective etching procedure described in Ref. [9].

to be between 10 nm < d < 40 nm. Hence, the layer thicknesses found for our reference process without in-situ oxidation "Ref 2nd dep" are in accordance with those found by Chen et al., although Chen et al. investigated processes without second PSG deposition.

In contrast, d_{SiO2} for the process "in-situ thin" in Fig. 3 is significantly larger with $d_{SiO2} = (19 \pm 2)$ nm. This thicker intermediate SiO_2 layer is formed by the in-situ oxidation [9]. During in-situ oxidation, the oxygen from the atmosphere diffuses through the PSG and SiO_2 layers and reacts with the silicon at the surface to form SiO_2.

Attaching a second PSG deposition for process "in-situ thin 2nd dep", the second deposition clearly leads to an increase in d_{PSG} to $d_{PSG} = (23 \pm 1)$ nm, while d_{SiO2} is reduced to $d_{SiO2} = (12 \pm 2)$ nm. This result (i.e. the increase in d_{PSG} while d_{SiO2} is decreased) is in accordance with results we found in Ref. [9], where we investigated the influence of a second PSG deposition step on the PSG/SiO_2 stack layer for a diffusion process without in-situ oxidation. We propose that the reduction in d_{SiO2} results from the diffusion of phosphorus from the PSG layer to the PSG/SiO_2 interface, where they react with SiO_2 to form additional PSG [18]. The PSG layer thickness for process "in-situ thin 2nd dep" is comparable to that of the reference process.

Processes "in-situ thick" and "in-situ thick 2nd dep" feature significantly higher total layer thicknesses d than the other processes as the N_2-$POCl_3$ and O_2 gas flows during first PSG deposition are two to three times higher; see Table I. The strong first PSG deposition for "in-situ thick" results in a total thickness of $d \approx 70$ nm, while the weak first PSG deposition for the reference process and both "in-situ thin"-processes results in $d \approx 30$ nm. For diffusion "in-situ thick", $d_{SiO2} = (50 \pm 2)$ nm is more than twice as large as $d_{PSG} = (23 \pm 2)$ nm. The attached second PSG deposition for process "in-situ thick 2nd dep" hardly affects these layer thicknesses: $d_{SiO2} = (50 \pm 2)$ nm and $d_{PSG} = (27 \pm 2)$ nm. Only d_{PSG} is about 3 nm larger.

In contrast to the process "in-situ thin 2nd dep", d_{SiO2} is not decreased for process "in-situ thick 2nd dep" by adding the second PSG deposition step. As the intermediate SiO_2 layer is more than twice as thick for "in-situ

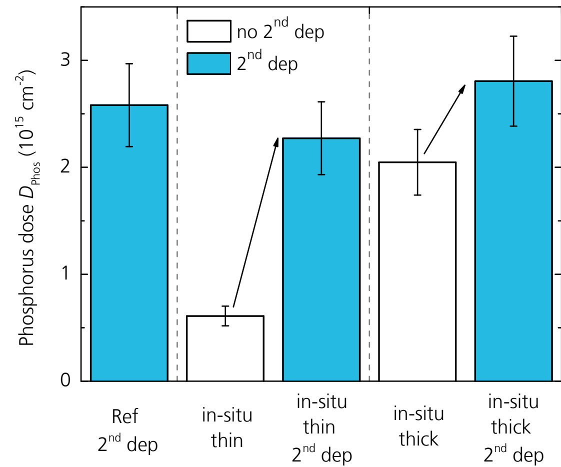

Figure 4: Total phosphorus dose within the PSG/SiO_2 stack layer for $POCl_3$ diffusion processes with and without second deposition step, determined by ICP-OES.

thick", it seems that there is either a critical SiO_2 layer thickness, which represses the increase of d_{PSG} by a second deposition step, or a critical PSG layer thickness, from which point the PSG layer growth occurs slower.

Also remarkable is the fact that for all processes that feature the (same) second deposition step, similar d_{PSG} values between 23 nm $\leq d_{PSG} <$ 27 nm are found, irrespective on the gas flows used during first deposition and drive-in. On the other hand, d_{SiO2} varies significantly between 6 nm $\leq d_{SiO2} <$ 50 nm.

3.2 Phosphorus dose of the PSG/SiO_2 stack layers

The phosphorus dose within the total PSG/SiO_2 stack layers on textured surface is determined by ICP-OES. The ICP-OES measurement gives the phosphorus weight within the examined solution in µg/l. This quantitiy is converted to the amount of phosphorus atoms and then divided by the sample area. As the diffusion occurs on both wafer surfaces, that value is further divided by two to obtain the phosphorus dose D_{Phos} for one wafer side.

Fig. 4 shows the obtained phosphorus doses D_{Phos} for the five diffusion processes. It is evident that the second PSG deposition step leads to significantly higher D_{Phos} that ranges between $(2.3 \pm 0.3)\cdot 10^{15}$ cm$^{-2} \leq D_{Phos} \leq (2.8 \pm 0.4)\cdot 10^{15}$ cm^{-2}. For process "in-situ thin", the second deposition leads to an increase in D_{Phos} from $D_{Phos} \approx (0.61 \pm 0.09)\cdot 10^{15}$ cm^{-2} to $D_{Phos} \approx (2.3 \pm 0.3)\cdot 10^{15}$ cm^{-2}, which corresponds to a factor of four. Process "in-situ thick" with very thick intermediate SiO_2 layer, see Fig. 3, shows a slighter increase in D_{Phos} due to the second deposition step. This is consistent with the assumption that the majority of the phosphorus is located in the PSG layer [9,18] and hence a slight increase in d_{PSG} correlates with a slightly higher D_{Phos}.

3.3 Phosphorus doping profiles after $POCl_3$ diffusion

Fig. 5(a) shows the as-diffused charge carrier concentration profiles of the reference process and the two diffusion processes "in-situ thin" and "in-situ thin 2nd dep", determined by ECV measurements on textured surface. The profile depth d_{prof} at a dopant concentration $N = 10^{17}$ cm^{-3} is between 320 nm < d_{prof} < 400 nm. It is clear that the surface charge carrier concentration $N_{surf} = (6.5 \pm 0.7)\cdot 10^{19}$ cm^{-3} for the reference process "Ref 2nd dep" is lower than for the "in-situ thin"-process with $N_{surf} = (2.1 \pm 0.2)\cdot 10^{20}$ cm^{-3}. On the other hand, the course of the profiles for processes

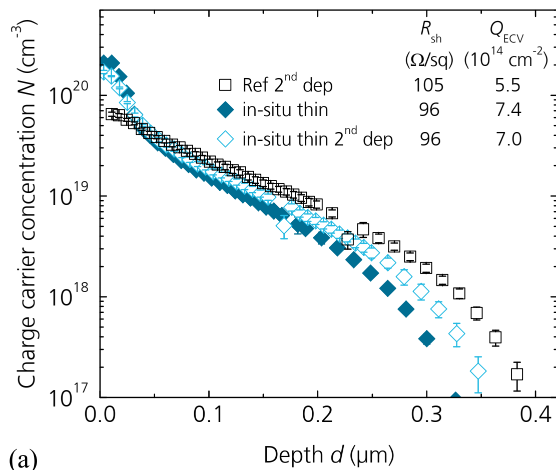

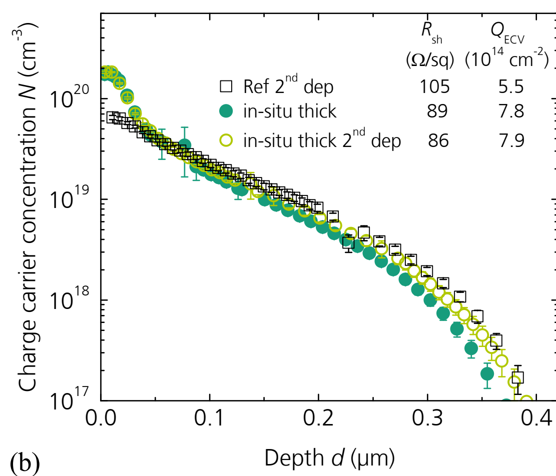

Figure 5: Charge carrier concentration profiles obtained by the ECV technique after PSG etching on textured surface for the five diffusion processes stated in (a) and (b). The emitter sheet resistances R_{sh} as well as the integrated total charge carrier dose Q_{ECV} are stated.

"in-situ thin" and "in-situ thin 2nd dep" is very similar. Hence, the performed second deposition step hardly affects the resulting doping profile. This is confirmed by the integrated total charge carrier dose Q_{ECV} given in Fig. 5(a), which is similar for both processes within the measurement uncertainty.

Although the PSG/SiO_2 layer thicknesses are very similar for the processes "Ref 2nd dep" and "in-situ thin 2nd dep" (Fig. 3), the courses of the profiles are different.

Fig. 5(b) shows the charge carrier concentration profiles of, the reference process and the two diffusion processes "in-situ thick" and "in-situ thick 2nd dep". Here, d_{prof} is very similar for all processes with $d_{prof} \approx 400$ nm. Both "in-situ thick"-processes with $N_{surf} = (1.8 \pm 0.2)\cdot 10^{20}$ cm^{-3} result in very similar charge carrier concentration profiles as obtained for the two "in-situ thin"-processes. Again, it is clear that the performed second deposition step hardly affects the resulting doping profile: the charge carrier concentrations are very similar either without or with second deposition. This is also confirmed by the integrated total charge carrier dose Q_{ECV} given in Fig. 5(b), which is similar for both processes.

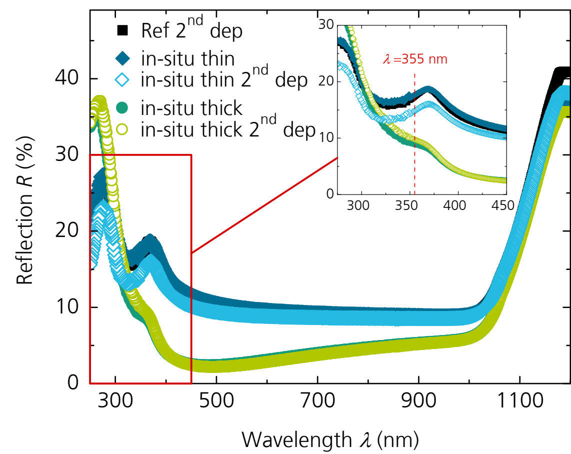

Figure 6: Reflection measurements on textured surface with the PSG/SiO_2 stack layers from the indicated $POCl_3$ diffusion processes.

3.4 Impact of laser doping on sheet resistance

As the laser doping process is at least partly dependent on the coupling of the laser radiation into the silicon material, the absorption A of the samples is of interest. In order to obtain A, we measure the reflection R which is dependent on the surface morphology and the total layer thickness of the PSG/SiO_2 stack. Commonly, lasers with wavelengths between 355 nm $\leq \lambda_{laser} \leq$ 1030 nm are used for laser doping approaches [23]. Within this work, we use a UV ns-laser at λ_{laser} = 355 nm.

Fig. 6 shows R as a function of wavelength λ. R is significantly lower at λ_{laser} = 355 nm for both "in-situ thick" diffusion processes compared to the other processes as they feature a thicker PSG/SiO_2 stack layer. As the transmission is zero for λ_{laser}, the absorption is $A = 1 - R$. For the results plotted in Fig. 7, we multiplied the applied pulse energy $E_{P,set}$ with the corresponding A, in order to account for the differences in reflection. However, note that the reflectance changes dramatically during the application of each laser pulse due to local heating and melting of the wafer surface.

Fig. 7 summarizes the obtained sheet resistances $R_{sh,4pp}$, determined by 4pp measurements after laser doping. All three images (a) to (c) have in common that $R_{sh,4pp}$ decreases continuously with increasing E_P. For the reference $POCl_3$ diffusion process with second deposition "Ref 2nd" (no in-situ oxidation) in Fig. 7(a), $R_{sh,4pp}$ is reduced from $R_{sh,4pp} \approx 100$ Ω/sq to $R_{sh,4pp} \approx 20$ Ω/sq if E_P is increased to $E_P \approx 100$ µJ. For both diffusion processes with in-situ oxidation and second deposition in Fig. 7(a), also a significant reduction in $R_{sh,4pp}$ to $R_{sh,4pp} \approx 25$ Ω/sq and $R_{sh,4pp} \approx 30$ Ω/sq is seen for the processes "in-situ thin 2nd dep" and "in-situ-thick 2nd dep", respectively. However, the reductions in $R_{sh,4pp}$ are somewhat weaker pronounced than for the reference.

Referring to Figs. 3 and 4, it is clear that the different thicknesses of the intermediate SiO_2 layer is the dominating property which causes the differences in the obtained $R_{sh,4pp}$ values after laser doping in Fig. 7(a), as all three $POCl_3$ diffusion processes feature comparable d_{PSG} and D_{Phos}. The thicker the intermediate SiO_2 layer is, the less is the achievable reduction in $R_{sh,4pp}$. The presence of a thick intermediate SiO_2 layer ($d_{SiO2} \approx 50$ nm) thus retards the in-corporation of phosphorus from the PSG layer into the silicon surface considerably compared to the thinner SiO_2 layer ($d_{SiO2} \approx 12$ nm) present for the "in-situ thin

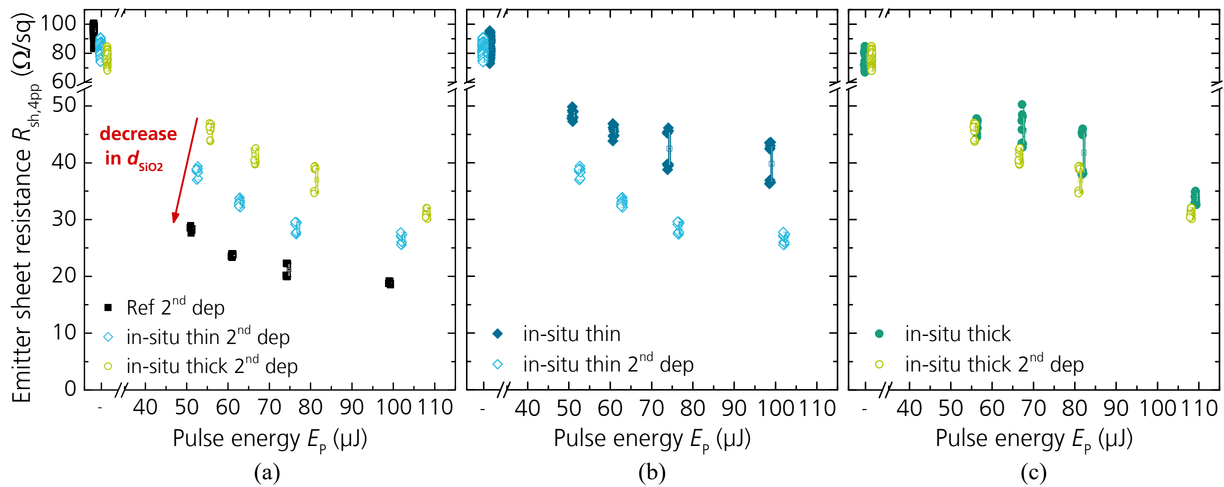

Figure 7: Emitter sheet resistances $R_{sh,4pp}$ after laser doping for the pulse energies E_P—which correspond to the applied pulse energies $E_{P,set}$ times the absorption A—of the respectively indicated diffusion processes in (a) to (c). The pulse-to-pulse as well as the line-to-line distance is constant for all E_P. One hundred 4pp measurements are performed for all diffusion processes without laser doping (-), while ten 4pp measurements are performed per E_P and per diffusion process.

2nd dep" diffusion process. The even thinner intermediate SiO_2 layer ($d_{SiO2} \approx 6$ nm) of the reference process allows for an even stronger laser doping.

Fig. 7(b) shows the impact of the second deposition step during $POCl_3$ diffusion for the "in-situ thin" processes. Obviously, the second deposition and thus, the higher D_{Phos} as shown in Fig. 4, allows for significantly higher doping resulting in lower $R_{sh,4pp}$ values. Remember that the second deposition step not only increases D_{Phos} but also leads to the decrease in the intermediate SiO_2 layer thickness; see Fig. 3. A thinner SiO_2 layer also allows for higher laser doping, compare Fig. 7(a).

For the "in-situ thick" processes in Fig. 7(c), $R_{sh,4pp}$ decreases with increasing E_P, but only slightly lower values are seen for the $POCl_3$ diffusion process with second deposition at each E_P. This can be explained by the only slight increase of the phosphorous dose due to the second deposition (see Fig. 4). The thick intermediate SiO_2 layer (see Fig. 3) seems to prevent the in-diffusion of phosphorus atoms from the PSG into the silicon for both "in-situ thick" processes, although slightly more phosphorus is provided within the PSG/SiO_2 stack layer for "in-situ thick 2nd dep" (see Fig. 4).

5 SUMMARY AND CONCLUSION

Five different diffusion processes utilizing phosphorus oxychloride ($POCl_3$) as liquid dopant precursor are examined with respect to their as-diffused properties and their suitability with laser doping from phosphosilicate glass (PSG) to form a selective emitter structure. Therefore, variations in deposition parameters, in-situ oxidation (e.g. high oxygen flow during drive-in), and the influence of a second PSG deposition step (e.g. active N_2 flow through the $POCl_3$ bubbler after drive-in) are investigated.

The $POCl_3$ diffusions with in-situ oxidation result in grown stack layers consisting of silicon dioxide (SiO_2) and PSG, whose intermediate SiO_2 layers with a thickness $d_{SiO2} = (19 \pm 2)$ nm or $d_{SiO2} = (50 \pm 2)$ nm are twice as thick as the PSG layers with thicknesses $d_{PSG} = (10 \pm 1)$ nm and $d_{PSG} = (23 \pm 1)$ nm, respectively. The total PSG/SiO_2 stack layer thickness depends on the chosen gas flows during deposition. The higher $POCl_3$ and O_2 gas flows result in thicker stack layers.

The implementation of a second PSG deposition step for the diffusion process with in-situ oxidation results in increased PSG layer thicknesses, while the charge carrier concentration profiles hardly change. The SiO_2 layer thickness decreases if the intermediate SiO_2 layer before second deposition does not exceed a critical thickness. Or, there is a critical PSG layer thickness from which the PSG layer growth occurs slower. The reference $POCl_3$ diffusion without in-situ oxidation but with second deposition features a thin SiO_2 with $d_{SiO2} = (6 \pm 2)$ nm, while the PSG layer is about four times thicker.

We find that the $POCl_3$ diffusion processes with second PSG deposition feature a higher total phosphorus dose D_{Phos} within the PSG/SiO_2 stack layers. D_{Phos} ranges between $(2.3 \pm 0.3)\cdot 10^{15}$ cm$^{-2} \leq D_{Phos} \leq (2.8 \pm 0.4)\cdot 10^{15}$ cm^{-2} for all processes with second deposition.

Laser doping applied to the PSG/SiO_2 stack layers reduces the emitter sheet resistance R_{sh} with increasing laser pulse energy. It is found that for the $POCl_3$ diffusion processes with second PSG deposition, R_{sh} can be significantly more reduced compared with the $POCl_3$ diffusion processes without second deposition as long as the intermediate SiO_2 layer thickness is a few 10 nm or less. From $R_{sh} \approx 90$ Ω/sq after diffusion, R_{sh} can be reduced to 15 Ω/sq $< R_{sh} <$ 35 Ω/sq by laser doping. This result suggests that the additionally provided phosphorus from the second deposition step is advantageous for laser doping. For $POCl_3$ diffusion processes with in-situ oxidation, the reduction in R_{sh} by the laser process is weaker for thicker intermediate SiO_2 layers. For SiO_2 layer thicknesses above about 50 nm, laser doping results in similar R_{sh} values measured on samples either diffused with or without second PSG deposition step.

In summary, our results show that $POCl_3$ diffusion processes with in-situ oxidation are suitable for the formation of selective emitters by laser doping.

ACKNOWLEDGEMENTS

The authors would like to thank all colleagues at the Fraunhofer ISE PV-TEC; especially C. Harmel for laser

processing, A. Fischer and S. Maus for selective etching, A. Moldovan for ICP-OES measurements, S. Schmidt and S. Dholipet Nagendra Kumar for ECV measurements and M. Berlin for 4pp measurements. This work was funded by the German Federal Ministry for Economic Affairs and Energy within the research project “POLDI” under contract number 0324079D.

REFERENCES

[1] ITRPV, 2017, "International Technology Roadmap for Photovoltaic (ITRPV) - Results 2016", available onl.: http://www.itrpv.net/Reports/ Downloads/2017/.

[2] A. Cuevas, "A good recipe to make silicon solar cells", *Proc. 22nd IEEE PVSC*, Las Vegas, USA, 1991, pp. 466–470.

[3] A. Kimmerle, R. Woehl, A. Wolf et al., "Simplified front surface field formation for back contacted silicon solar cells", *Energy Proced.*, vol. 38, pp. 278–282, 2013.

[4] S. Werner, E. Lohmüller, S. Maier et al., "Process optimization for the front side of p-type silicon solar cells", *Proc. 29th EU PVSEC*, Amsterdam, The Netherlands, 2014, pp. 1342–1347.

[5] S. Werner, E. Lohmüller, A. Wolf et al., "Extending the limits of screen-printed metallization of phosphorus- and boron-doped surfaces", *Sol. Energy Mater. Sol. Cells*, vol. 158, pp. 37–42, 2016.

[6] T. Dullweber, H. Hannebauer, S. Dorn et al., "Emitter saturation currents of 22 fA/cm^2 applied to industrial PERC cells approaching 22% conversion efficiency", *Proc. 32nd EU PVSEC*, Munich, Germany, 2016, pp. 335–339.

[7] A. Wolf, A. Kimmerle, S. Werner et al., "Status and perspective of emitter formation by $POCl_3$-diffusion", *Proc. 31st EU PVSEC*, Hamburg, Germany, 2015, pp. 414–419.

[8] P. A. Basore, J. M. Gee, M. E. Buck et al., "Simplified high-efficiency silicon cell processing", *Proc. 7th Int. PVSEC*, Nagoya, Japan, 1993, pp. 61–64.

[9] S. Werner, S. Mourad, W. Hasan et al., "Structure and composition of phosphosilicate glass systems formed by $POCl_3$ diffusion", *Energy Proced.*, in press, 2017.

[10] A. W. Blakers, A. Wang, A. M. Milne et al., "22.8% efficient silicon solar cell", *Appl. Phys. Lett.*, vol. 55, no. 13, pp. 1363–1365, 1989.

[11] S. Werner, E. Lohmüller, P. Saint-Cast et al., "Key aspects for fabrication of p-type Cz-Si PERC solar cells exceeding 22% conversion efficiency", *Proc. 33rd EU PVSEC*, Amsterdam, The Netherlands, 2017.

[12] P. Saint-Cast, S. Werner, J. Greulich et al., "Analysis of the losses of industrial-type PERC solar cells", *Phys. Status Solidi A*, 2016.

[13] S. Werner, E. Lohmüller, S. Maier et al., "Challenges for lowly-doped phosphorus emitters in silicon solar cells with screen-printed silver contacts", *Energy Proced.*, in press, 2017.

[14] G. Fischer, M. Müller, S. Steckemetz et al., "Model based continuous improvement of industrial p-type PERC technology beyond 21% efficiency", *Energy Proced.*, vol. 77, pp. 515–519, 2015.

[15] M. Müller, B. Bitnar, G. Fischer et al., "Loss analysis of 22% efficient industrial PERC solar cells", *Energy Proced.*, in press, 2017.

[16] L. Ventura, A. Slaoui, J. C. Muller, "Realization of selective emitters by rapid thermal and laser assisted techniques", *Proc. 13th EU PVSEC*, Nice, France, 1995, pp. 1578–1581.

[17] A. Cuevas, P. A. Basore, G. Giroult-Matlakowski et al., "Surface recombination velocity of highly doped n-type silicon", *J. Appl. Phys.*, vol. 80, no. 6, pp. 3370–3375, 1996.

[18] R. Chen, H. Wagner, A. Dastgheib-Shirazi et al., "A model for phosphosilicate glass deposition via $POCl_3$ for control of phosphorus dose in Si", *J. Appl. Phys.*, vol. 112, no. 12, p. 124912, 2012.

[19] Nölte, Joachim, "ICP - Emissionsspektrometrie für PraktikerWiley, 2002.

[20] E. Peiner, A. Schlachetzki, D. Krüger, "Doping profile analysis in Si by electrochemical capacitance-voltage measurements", *J. Electrochem. Soc.*, vol. 142, no. 2, pp. 576–580, 1995.

[21] R. Bock, P. P. Altermatt, J. Schmidt, "Accurate extraction of doping profiles from electrochemical capacitance voltage measurements", *Proc. 23rd EU PVSEC*, Valencia, Spain, 2008, pp. 1510–1513.

[22] U. Jäger, S. Mack, C. Wufka et al., "Benefit of selective emitters for p-type silicon solar cells with passivated surfaces", *IEEE J. Photovoltaics*, vol. 3, no. 2, pp. 621–627, 2013.

[23] U. Jäger, M. Okanovic, M. Hörteis et al., "Selective emitter by laser doping from phosphosilicate glass", *Proc. 24th EU PVSEC*, Hamburg, Germany, 2009, pp. 1740–1743.